LANGMUIR

pubs.acs.org/Langmuir Article

Will Polycrystalline Platinum Tip Sliding on a Gold(111) Surface Produce Regular Stick—Slip Friction?

Rong-Guang Xu, Gunan Zhang, Yuan Xiang, Jonathan Garcia, and Yongsheng Leng*



Cite This: Langmuir 2022, 38, 6808-6816



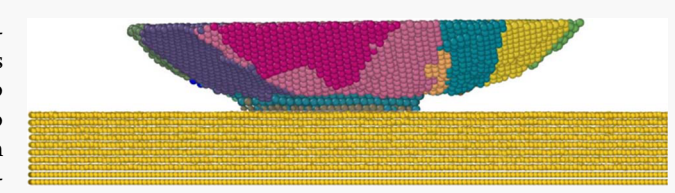
ACCESS

Metrics & More



SI Supporting Information

ABSTRACT: Friction measurements by an atomic force microscope (AFM) frequently showed regular stick—slip friction signals with atomic-scale resolutions. Typically, for an AFM metal tip sliding on a metal crystal surface, the microstructure of the tip made from the thermally evaporated metal coating on a silicon cantilever was polycrystalline. Our detailed molecular dynamics-(MD) simulations of a polycrystalline Pt tip (R = 10 nm in radius)



sliding on an Au(111) surface revealed how the geometry of the polycrystalline tip took effect on the friction behavior at the contact interface. We found that the apex of the Pt tip with multiple grains near the edge of contact could induce severe plastic deformations of the gold substrate, leading to irregular stick—slip frictions upon sliding. Simulation results showed that in order to achieve a clear stick—slip friction signal with single atomic slips, the apex of the Pt tip must adopt a single crystalline protrusion without any neighboring grains involved in the metal contact. We showed that such a single crystalline protrusion, which presumably could be achieved during initial run-in or wear-out of high-energy Pt atoms in the neighboring grains, was passivated by a large number of gold atoms due to metal adhesion in the contact periphery. Using such a crystalline protrusion tip, we demonstrated that the stick—slip friction produced was very "tolerant" to the adhesion of a large number of gold atoms on the tip apex. We further showed that AFM tip mass used in MD simulations also played an important role in determining the transition between friction regimes, which could be well explained by the Prandtl—Tomlinson thermal activation model.

1. INTRODUCTION

Atomic force microscope (AFM)¹ can be operated as a friction force or scanning force microscope² to investigate friction in a single asperity contact at nanoscales. Experimental advances in AFM have enabled friction measurements and characterizations of an AFM metal tip sliding on a metal surface with atomic resolutions. Such a dramatic achievement in AFM experimentation provides a powerful tool for the study of fundamental science in nanoscale friction,^{3,4} especially stick—slip motion and energy dissipation in nanotribology contacts. One of the benefits from AFM friction measurements is that atomic stick—slip friction signals are frequently used to map the atomic features of the surface, i.e., the friction map reflects the topography of the scanned surface.

Theoretical and computational studies of nanoscale friction^{3–22} provide critical insights into this phenomenon that otherwise cannot be revealed barely through AFM experimentations. In particular, molecular dynamics (MD) simulations have been used as a predictive tool to complement AFM experimentation by investigating the detailed atomic motions at the contact interface between an AFM tip and a substrate surface even at the buried interface not accessible to current experimental instruments. Early MD simulation studies by Sorensen et al. investigated atomic-scale sliding friction of a tip—surface contact.¹³ The stick—slip friction of a single crystalline Cu tip on a Cu (111) surface occurred due to the elastic bending deformation of the tip under constant velocity

sliding motion or a quasi-static motion of the tip. A more realistic simulation model for the stick—slip motion of an AFM tip is to add driving springs directly to the tip to represent the elasticity of the AFM cantilever. This approach was implemented in some of previous MD simulation studies for nanoscale friction^{4,20–22} and has been developed as a fix command in the LAMMPS (large-scale atomic/molecular massively parallel simulator) package.²³

Atomic friction on gold surfaces attracts much interest because it exhibits the most interesting frictional properties on the nanometer scale.²⁴ These studies include load dependence of kinetic friction by Gosvami et al.^{25,26} and speed dependence of atomic stick—slip friction by Li et al.,²⁰ in which the MD and AFM conditions are controlled to match as closely as possible. Interfacial sliding friction in gold nanojunctions was also reported recently²⁷ in which atomic rheology was measured to evaluate energy dissipation behavior at this extreme scale. Gosvami et al. also studied temperature effect on kinetic friction.²⁵ They found that stable stick—slip friction was only

Received: December 7, 2021 Revised: May 10, 2022 Published: May 26, 2022





weakly dependent on the temperature between 300 and 170 K, and below 170 K, friction was increased with time and a distortion of the stick—slip characteristic was observed. A relevant research study done by Ko et al. found that for the miscible metal couples such as a Pt—Au contact, the friction is governed by high adhesion, while the shear strength is low. However, for immiscible metal couples such as a Pt—Ag contact, adhesion is found to be low, and the shear strength is high. They also found that the periodicity of atomic stick—slip images corresponds to the interatomic distance of gold for immiscible counter-bodies, whereas for miscible couples (such as Pt—Au contact), the periodicity of atomic stick—slip significantly differs from the gold interatomic distance and may correspond to the structural length of an ordered intermediate phase at the tip—surface interface.

A challenging issue in MD simulation of atomic-scale friction in AFM is that a well-defined contact geometry between the AFM tip apex and the sample surface is difficult to determine and is usually unknown. This problem has recently been investigated through transmission electron microscopy (TEM) coupled with matched MD simulation to determine the loaddependent size of a platinum nanocontact.²⁹ A direct real-time observation of the atomic-scale friction between a W tip sliding on an Au(111) tip was carried out recently through in situ high-resolution TEM and AFM measurements.³⁰ This study showed the formation of a loosely packed interfacial layer between two metallic asperities that enabled a diffusionmediated low friction under tensile stress. Since the tip contact geometry only allows small back-and-forth sliding from a full contact to an almost-zero contact, it is not clear if the long distance nanoscale friction could be studied using the same experimental method especially during the stable stick-slip motion of the AFM tip on a flat substrate surface.

An important work using combined experimental and accelerated MD simulation studies on the nanoscale friction of an AFM Pt tip sliding on an Au(111) surface was reported by Li et al.²⁰ Because it is very difficult to determine the atomic structure of the Pt tip's surface experimentally, only the apex of the tip is modeled as a single crystal in this study, which is a common practice in many MD simulations to model crystal metal tips. The similar stick—slip friction dynamics observed in both AFM friction measurements and MD simulations, but at very different time scales, are largely attributed to the same energetics at the contact interface.²⁰ However, the very small tip mass associated with hundreds of Pt atoms in the model tip results in very different attempt frequencies of friction slips.²⁰

It is generally believed that the geometry and structure of a probe tip can quantitatively influence friction results because the interaction between the tip and the scanned surface is very sensitive to the atomic structure of the tip. Whereas several MD simulation control parameters, such as estimated contact area, sliding orientation, normal load, temperature, and driving spring constants, etc., can be selected to match AFM calibrated parameters as closely as possible, 20,31 the uncertainty of tip geometry and atomic structure, especially at the tip apex, makes the quantitative comparison between simulation and experimental results challenging. Typically, the atomic structure of an AFM Pt tip made from thermally evaporated Pt coating on a silicon cantilever is polycrystalline.²⁰ In a more realistic situation, the apex of the metal tip might consist of a major single grain with a few neighboring grains coupled together.2

In this work, we examine the atomic-scale friction of a polycrystalline Pt metal tip sliding on an Au(111) surface by carrying out straightforward MD simulations. The motivation to select this model system is because (1) platinum tips are widely used in probe-based microscopy, (2) in nanoscale electronics devices, Pt and Au are two commonly used electrodes, and (3) gold surfaces exhibit the most interesting frictional properties on the nanometer scale. An R = 10 nm radius polycrystalline Pt tip has been built and employed in this study. We emphasize that since this is a quite large Pt tip (the tip apex has over 18,000 Pt atoms) compared to previous model tips used in MD simulations, 20,31 in order to observe sliding friction in the MD time regime, a detached tip mass equivalent to a few hundred to thousand metal atoms has to be used. This is realized by employing a two-step MD simulation procedure that can be implemented in LAMMPS²³ (Section 2). However, such a simulation approach brings in an additional effect, the dynamic inertia of the AFM model tip that may inadvertently change the stick-slip dynamics of nanoscale friction. This will be discussed in detail in Section 3.

A previous experimental study showed that transitions from single-slip to multiple-slip regimes in atomic-scale friction depend on the lateral stiffness of the coupled tip—substrate system and contact load, 32 while the effective mass of the AFM tip—cantilever system is constantly around $10^{-11}~{\rm kg.}^{20,21}$ In MD simulations, however, one should keep in mind that properly selecting a dynamic inertia of the model tip is not only a matter of choice but also an important control parameter in order to capture the critical dynamics and energetics in AFM friction simulations.

This paper is organized as follows: Section 2 is dedicated to the method descriptions of building the polycrystalline Pt tip and the friction simulation using a two-step MD approach; in Section 3, we present and discuss simulation results showing under what conditions (mainly concern about the atomic structure of the tip apex and tip mass) the stick—slip friction with single slips could be realized. We summarize our research with important conclusions in Section 4.

2. SIMULATION METHODS

2.1. Atomic Interaction Potential and Temperature Control in Simulations. The embedded atom method (EAM) with Voter's modifications³³ was employed for all interatomic interactions. Here, for Au–Pt interactions, the EAM electron density function was rescaled to identify a single summed electron density for fcc Pt and Au. An arithmetic mean of the pure material potentials was applied to model interactions between dissimilar atoms. Although this mixing rule may not be sufficient to reproduce the Au–Pt phase properties, the energetics of the Au–Pt binary contact and its nanoscale friction behavior was well represented.²⁰ A time step of 2.0 fs in MD simulations with the LAMMPS package²³ is used throughout this study. The temperature of the system is controlled by the Nosé–Hoover thermostat.^{34,35}

2.2. Building the Polycrystalline Pt Tip. In this work, a polycrystalline Pt tip with the grain size on the tip apex similar to that in ref 29 is constructed by a quench from the melt. The polycrystalline atomic structure is characterized by the OVITO visualization package 36 with the grain segmentation modifier. OVITO can identify individual grains in a polycrystalline microstructure by grouping atoms in crystal regions having similar local lattice orientations. The initial simulation box has an fcc single crystalline structure with the dimension of 17 nm \times 17 nm \times 17 nm, containing a total of 327,475 Pt atoms.

First, the system is heated to 2500 K to form a platinum sphere of $\sim 10\,$ nm in radius in liquid state. The polycrystalline Pt tip is

constructed in the following manner: (1) Starting from 2500 K, the system is cooled down from the melt with a 500 K decrease in every one million time steps (corresponding to the cooling rate of 2.5×10^7 K/s). This is followed by a further equilibrium run at constant temperature to relax the structure for another one million time steps; (2) The procedure is repeated until T = 500 K; (3) The system is then cooled down to 293 K in one million time steps, followed by an equilibrium run at 293 K for another one million time steps. The equilibrated Pt spherical particle of $R \approx 10$ nm in radius is shown in Figure 1a; (4) The Pt tip is made by cutting a spherical cap around a

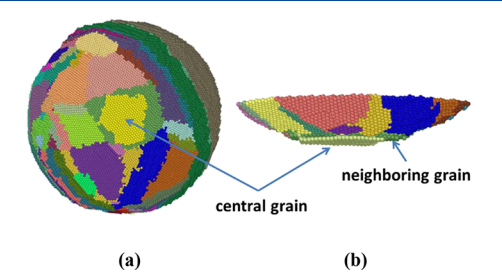


Figure 1. (a) R = 10 nm Pt spherical particle obtained by quench from a melt, and (b) final atomic configuration of the Pt tip apex.

central grain (shown in yellow in Figure 1a). The height of this spherical cap is around 2.6 nm, consisting of 18,364 Pt atoms; (5) Further MD relaxation of the Pt tip is carried out for one million time steps while keeping the topmost 0.5 nm of the probe as a rigid body. The final atomic structure of the Pt tip is shown in Figure 1b. Here, the contacting surface of the polycrystalline Pt tip apex is the (111) surface of the central grain. This surface initially contains roughly 350 Pt atoms, surrounded by the tilt (111) surfaces of neighboring grains.

2.3. Stable Contact between Polycrystalline Pt Tip and Au(111) Surface. The Au(111) substrate has a dimension of 20 nm \times 16 nm \times 1.9 nm with a crystallographic orientation of [111] in the z-direction. The x and y axes are along the [1 $\overline{10}$] and [11 $\overline{2}$] directions, respectively. Periodic boundary conditions are applied in both x- and y-directions. The gold substrate is relaxed at 293 K with the bottom two layers fixed.

Initial stable contact between the Pt tip and the gold(111) is established following four steps: (1) Freezing the whole Au substrate and the Pt tip and using a very hard spring (k = 150,000 N/m) to suspend the rigid tip about 4 Å above the Au(111) surface. It is found that the rigid Pt tip can rotate around its normal z axis to find a selfequilibrium position between the two rigid bodies. Such a selfadjusted contact conformation results in a Moiré contact pattern (Figure 2a), which was also discussed in previous MD simulation studies;³¹ (2) Pushing the hard spring slowly (0.1 m/s) to make the rigid Pt tip approach the Au(111) surface until the interaction force between the two bodies becomes slightly repulsive; (3) Relaxing the contacting system through MD equilibration. Adhesion and fast diffusion results in a large number of gold atoms jumping to the Pt tip, especially around the high-energy grain boundaries at the tip apex; (4) Replacing the "damaged" Au(111) substrate with a perfect crystal one and continuing MD equilibrium runs. It was seen that the fast diffusion of gold atoms from the substrate to the Pt tip assisted the occupation of high energy defects on Pt tip and produced specific contacting configurations. This result confirmed that gold atoms have a faster diffusion at room temperature than Pt atoms.³⁷ The procedure was similar to a run-in that was usually repeated several times until no additional atomic hopping from the gold substrate to the Pt tip was observed. Figure 2b,c shows the final atomic configuration of the contact from the top and side views. Due to the crystal orientation mismatch at the grain boundaries near the edge of contact, significant atomic displacements of some gold atoms from the fcc crystal lattice are clearly seen (Figure 2c).

To understand the defect patterns within the Pt tip and Au substrate in proximity, we employ the OVITO visualization package³⁶ to characterize the local structural environment of atoms by the

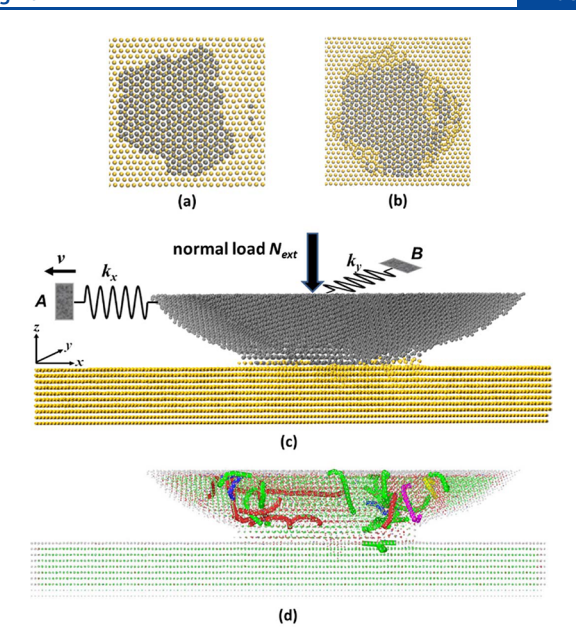


Figure 2. (a) Atomic contact in Moiré patterns between the bottom layer of the Pt tip and the top layer of the Au substrate before they are fully relaxed. (b) and (c) show the top and side views of the final atomic configuration of the Pt–Au contact after repeated equilibrations between the Au-attached Pt tip and Au(111) substrate. The MD simulation setup is shown in (c). (d) Snapshot of dislocation distribution in the polycrystalline tip and Au substrate. Blue, green, pink, yellow, cyan, and red lines represent perfect, Shockley partial, stair-rod, Hirth, Frank and other type of dislocations, respectively. Atoms in face-centered cubic (fcc), hexagonal close-packed (hcp), body-centered cubic (bcc), and other mixed crystalline structures are in green, red, purple, and white, respectively. The color scheme is consistent throughout this work.

polyhedral template matching (PTM) method³⁸ and monitor the dislocation movement by the dislocation extraction algorithm (DXA).^{39,40} The PTM method can identify local crystalline structures of simple condensed phases. The DXA can detect and analyze dislocations (including partial dislocations) in crystals through determining their Burgers vectors and displaying a line-based representation of the dislocation network. Figure 2d shows dislocation distributions in both polycrystalline tip and Au substrate. Different types of dislocations are represented by different colors. Atomic crystalline structures in different regions are also shown by different colors (see the caption of the figure). In particular, a Shockley partial dislocation line is formed at the top surface of the Au substrate, which is right below the two neighboring grains on the surface of the Pt tip. This signifies a plastic deformation in the Au substrate upon contacting the polycrystalline Pt tip.

2.4. Sliding Friction Simulation. During the sliding friction simulations, the bottom two layers of the gold substrate is fixed, and the topmost 0.5 nm thickness of the Pt tip is treated as a rigid body. The Pt tip is pulled along the x-direction by a driving spring (see Figure 2). The lateral spring constant is set to $k_x = 6$ N/m, while the stiffness of the spring along the y-direction ($k_v = 300 \text{ N/m}$) is much higher, making the motion of the tip along the axial direction of the cantilever largely constrained. The normal load of $N_{\rm ext}$ = 0.6 nN is applied to the top rigid layers of the Pt tip. These settings are consistent with previous AFM friction simulations.²⁰ The sliding speed is set to v = 1 m/s throughout simulations. Since the whole Pt tip is a very "heavy" tip consisting of 18,364 Pt atoms, to initiate sliding motion of the probe in MD time regime, a detached small tip mass, equivalent to $m_{\rm tip} = 100$ Au atomic mass, has to be used. This is realized by using a two-step MD simulation method that can be implemented in LAMMPS:2

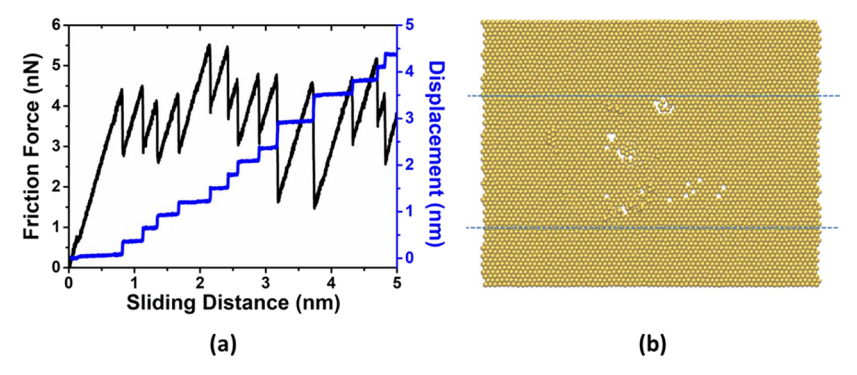


Figure 3. (a) Variations of the stick—slip friction force and actual displacement of the Pt tip versus the sliding distance of the driving spring. (b) Surface cavities and pile-up clusters of gold atoms on the top layer of Au(111) surface after the passage of the Pt tip. The two dashed lines in (b) indicate the friction trace of the bottom layer of the Pt tip in contact with the gold substrate.

- (i) Run one MD time step equilibration Δt , for the system with real atomic mass for both Au and Pt particles ($m_{\rm Au} = 197$ and $m_{\rm Pt} = 195$ amu), and calculate the total interfacial force applied to the Pt tip from the gold substrate $W_{\rm int}$, which is the summation of all individual atomic forces applied to the Pt tip;
- (ii) Evenly distribute the total interfacial force $W_{\rm int}$, the applied lateral spring force, $F_{\rm spring} = k(vt x)$, where x is the instantaneous tip position, and the external normal load $N_{\rm ext} = 0.6$ nN, to all Pt tip atoms. Simultaneously, reassign Pt atomic mass by evenly distributing the $m_{\rm tip} = 100$ Au mass to Pt atoms, which is equivalent to assigning an extremely small atomic mass close to the H atom (1.07 amu) to the Pt particles. Then, run one MD time step, Δt , for the Pt tip as a whole rigid body motion, followed by reassigning $m_{\rm Pt} = 195$ amu to Pt atom before going back to step (i) for the next round of MD trajectory propagations.

It should be noted that only in step (i) the temperature of the system is controlled at 293 K by a Nosé-Hoover thermostat. 34,3 This is the friction energy dissipation channel through atomic relaxations in both substrate and tip atoms. The energy dissipation rate is closely related to the atomic relaxation rate of the metal atoms. In step (ii), when the tip overcomes the energy barrier and proceeds to an unstable slip, the tip will impact the substrate atoms and generate phonons. These phonons are dissipated through atomic relaxation as heat in step (i) at a unique dissipation rate. Step (ii) is equivalent to solving the dynamics equations of motion of the Pt tip as a rigid body, i.e., $m_{\text{tip}}\ddot{x} = F_{\text{spring}} + W_{\text{int}} + N_{\text{ext}}$. This is directly carried out in LAMMPS using the run command with the default run_style verlet (velocity Verlet) algorithm. The two-step MD simulation is a more realistic friction simulation than the early MD simulation by Sorensen et al., 13 in which the Cu tip is either in a quasi-static or in a constant velocity sliding motion that cannot capture the stick-slip dynamics in AFM. However, varying the tip mass in step (ii) to proceed a rigid body motion of the whole tip, although it does not involve any atomic relaxation of the system, brings in an additional effect of the dynamic inertia of the AFM tip that may inadvertently influence the stick-slip friction dynamics, and eventually, the way of friction dissipation at the sliding interface. This has been recently discussed by van Baarle and Krylov et al.41 and will be further discussed in Section 3.

3. SIMULATION RESULTS AND DISCUSSIONS

3.1. Initial Sliding with High Stick—Slip Friction. Initial sliding simulations of the Pt tip along the x axis in both directions (forward- and backward-sliding) were carried out. As mentioned before, due to the crystal orientation mismatch at the grain boundaries near the edge of contact (Figure 2c), very high friction was observed along both directions due to the surface defects formation on gold. This is shown in Figure 3a in which a typical friction force versus distance shows

irregular stick-slips with both single slips and double slips. The actual tip displacement versus the sliding distance also shows these single and double slip jumps. A few snapshots of atomic configurations and distributions of dislocations in the stick phase are shown in Figure S1 in the Supporting Information. Here, plastic deformation in the form of Shockley partial dislocation in the Au substrate are seen during the stick stage, induced by the two neighboring grains in the polycrystalline Pt tip. Figure 3b shows surface defects in the form of surface cavities or pile-up clusters of gold atoms after the scanning of the Pt tip. It is known that the surface diffusion of atoms plays an important role in contact formation and healing of surface wear damage.²⁵ However, the timescale of healing on the surface is much longer than typical MD simulation timescales. Therefore, healing of surface defects is not observed in our present study. Clearly, even a local crystal orientation mismatch near the edge of contact between the Pt tip and the Au(111) could affect the frictional behavior and destroy the stable single-slip signals. Therefore, any irregular stick-slip pattern of high friction is a strong indication of the surface damage in the form of either shearing or plowing plastic deformations.²²

3.2. Stable Stick—Slip Friction with Single Crystalline Protrusion on the Tip Apex. The irregular stick—slip behavior due to the crystal orientation mismatch at the grain boundaries near the edge of contact and subsequent formation of surface defects after the passage of Pt tip indicate that any grain boundaries on the tip apex involved in the tip—substrate contact would inevitably lead to irregular stick—slip friction signals. This could be one source of friction irregularities observed in AFM. We therefore anticipate that in order to achieve a clear atomic stick—slip friction signal in single-slip regime, the apex of the Pt tip must adopt a single crystalline protrusion without any neighboring grains involved at the contact interface. Such a single crystalline protrusion could be achieved during the initial run-in or wear-out of high energy Pt atoms near the grain boundaries.

With this anticipation, we trimmed the neighboring grains on the Pt tip by removing high-energy Pt atoms near the edge of contact, leaving a single crystalline protrusion on the tip apex. This is shown in Figure 4a in which the tip—substrate contact was further equilibrated by an additional 500 ps MD equilibrium run. A large number of gold atoms near the edge of the Pt single crystalline protrusion were seen due to strong metal adhesions. Here, the contact area involves 342 Pt atoms and 117 attached Au atoms.

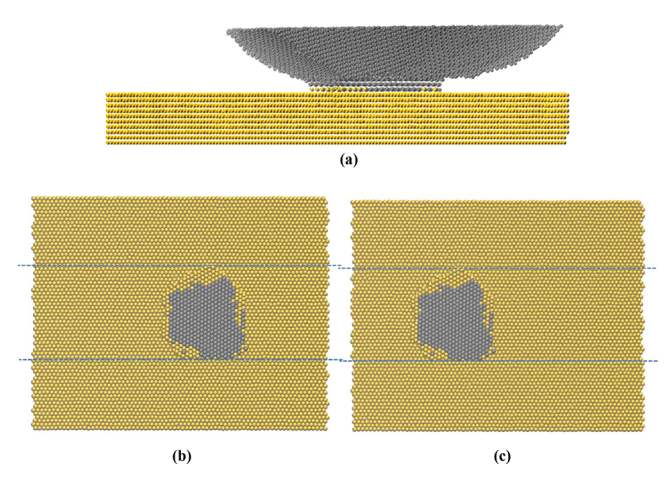


Figure 4. (a) Final Pt tip—Au(111) equilibrium contact after trimming the high-energy Pt atoms near the edge of contact. (b) Initial and (c) final atomic configuration of the bottom layer of the Pt tip and the top layer of the Au substrate after one forward-sliding friction simulation. The two blue lines highlight the moving track of the Pt tip, together with a large number of attached gold atoms near the edge of Pt single crystalline protrusion.

Subsequent friction simulations of the Pt tip sliding on a perfect Au(111) surface without any surface defects were carried out. Here, although there were a large number of attached gold atoms on the edge of tip protrusion (Figure 4), a regular sawtooth-like stick—slip friction force was observed, with the lateral displacement of the tip showing single-slip cycles (Figure 5). The periodicity of these single slips was

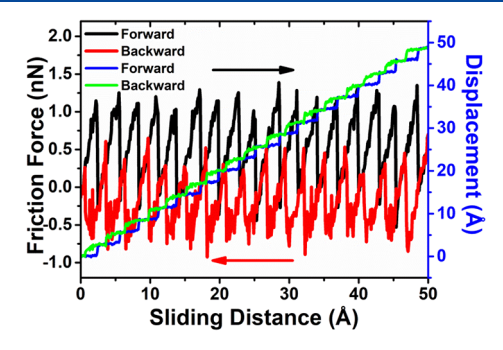


Figure 5. Stick—slip friction force loop and variations of the lateral displacements of the Pt tip versus the sliding distance of the driving spring.

around 0.28 nm, corresponding to the first neighbor distance between two gold atoms on the Au(111) surface. The regular stick—slip friction indicated that no surface defects were further created during sliding friction, which was confirmed by the sequential snapshots of the contacting interface (Figure 4b,c). We considered this regular stick—slip friction between the Pt tip and the Au substrate as purely elastic because no further atomic transfers between the tip and the substrate were observed. Such regular stick—slip friction signals were very robust in the subsequent forward—backward tip scanning, demonstrating that the stick—slip friction was very "tolerant" to the adhesion of a large number of gold atoms on the tip apex. In contrast to the finding by Ko et al., ²⁸ our results show that even for the miscible reactive Pt—Au contact, the periodicity of atomic stick—slip friction still corresponds to the interatomic distance of gold(111) surface.

The purely elastic stick-slip friction can be further confirmed from dislocation motion analysis. In contrast to the irregular stick-slip high friction due to plastic deformation (Section 3.1), we did not observe any form of dislocation initiation or atomic rearrangements at the sliding interface (see Figure S2 in the Supporting Information). The slightly dynamic evolutions of different types of dislocations within the Pt tip were attributed to elastic shifts of Pt atoms in the grain boundaries. Force fluctuations in the stick phase (Figure 5) were purely associated with mechanical vibrations of the driving spring. Dislocation glides through the contact and, selfannihilates during the slip were not observed. These stable stick-slips correspond to the so-called "rigid slip" regime in which all atoms move coherently. 42 We attribute this to the small contact area between the Pt tip and the Au substrate, which involves 342 Pt atoms and 117 Au atoms at the sliding interface (Figure 4).

3.3. Effect of the Tip Mass on Stick—Slip Friction. As has been discussed previously, varying the tip mass or its dynamic inertia in MD friction simulations will inadvertently change the stick-slip dynamics of the AFM model tip and, eventually, the way of friction dissipation at the sliding interface. This was shown in Figure 6 from which we found that the stick-slip friction dynamics was changed from singleslip to multiple-slip friction regimes as the tip mass $m_{
m tip}$, was increased from 100 to 5000 Au mass. Here, we employed the same sliding speed of v = 1 m/s and the normal load of $N_{\text{ext}} =$ 0.6 nN. Stick-slip friction involving double slips began to occur for $m_{\rm tip} = 500$ Au mass tip. As the tip mass was gradually increased, more frequent double slips were seen. We found that these double slips were rarely associated with inelastic events such as atomic transfers between the tip and the gold substrate. More interestingly, the mean friction force was found to decrease as more double slips occurred (Figure 6).

Such a tip mass-dependent stick—slip friction transition could be modeled and explained by the Prandtl—Tomlinson (PT) model, 43,44 which has been widely used to interpret the physics of sliding friction, especially the thermally activated, velocity dependent friction. An extensive review on the PT model and its applications was given by Dong et al. Here, the friction dynamics of the tip motion could be described by a Langevin dynamics, viz.

$$m\ddot{x} + m\mu\dot{x} = -\frac{\partial V(x, t)}{\partial x} + \xi(t) \tag{1}$$

where m is the tip mass and μ is the viscous friction coefficient $(\mu = 2\gamma \sqrt{k/m})$, whereas the damping coefficient $\gamma = 1$ corresponds to the critical damping) and $\xi(t)$ is the random thermal activation force, satisfying the fluctuation—dissipation theorem, with its zero mean $\langle \xi(t) \rangle = 0$ and δ correlated

$$\langle \xi(t)\xi(t')\rangle = 2m\mu k_{\rm B}T\delta(t-t') \tag{2}$$

Here, $k_{\rm B}$ denotes the Boltzmann constant and T is the temperature. The random force and the damping term in eq 1 arise from the interactions between the model tip and the substrate in the form of phonons and/or other fast excitations that are not treated explicitly.⁴

The total potential energy of the system V(x, t) can be written as

$$V(x, t) = -\frac{U}{2}\cos\left(\frac{2\pi x}{a}\right) + \frac{1}{2}k(vt - x)^{2}$$
(3)

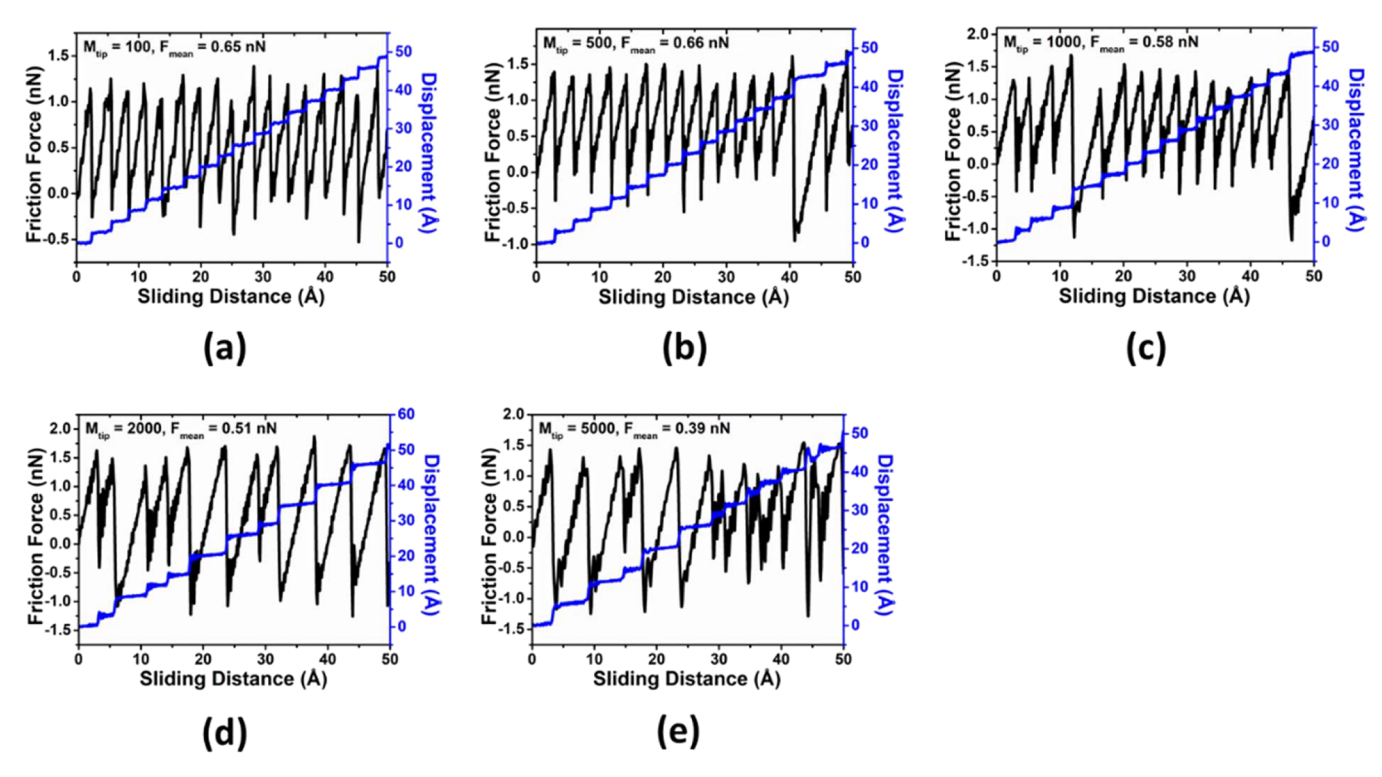


Figure 6. Variations of stick—slip friction force and tip displacement versus the sliding distance of the driving spring, for different tip masses varying from (a) $m_{\rm tip} = 100$ gold atomic mass, to (e) $m_{\rm tip} = 5000$ gold atomic mass. Mean friction forces are also shown in (a) to (e).

where U is the amplitude of the periodic corrugation potential induced by substrate, a is the lattice constant of the substrate, v is the sliding speed of the driving spring, and k is its spring constant.

We emphasize that in MD simulation since the stiffness of the spring along the y-direction ($k_y = 300 \text{ N/m}$) is much larger than that along the sliding direction ($k_x = 6 \text{ N/m}$), the movement of the Pt tip along the y-direction is largely constrained (Section 2.4). This computational setup is basically consistent with AFM friction measurements, in which the spring constant of the cantilever along its axial direction should be much larger than its lateral torsional force constant. Therefore, the one dimensional (1D) PT model is appropriate.

A critical question in the PT model is relevant to the determination of the damping coefficient (γ) or the viscous friction coefficient (μ) in eq 1. In the two-step MD simulation (Section 2.4), friction energy dissipation is proceeded in step (i) through atomic relaxations in both substrate and tip atomic particles. These particles have an intrinsic atomic relaxation rate $r_{\rm at} \approx \sqrt{\frac{k_{\rm at}}{m_{\rm at}}}$, where $k_{\rm at}$ is the typical binding spring constant and $m_{\rm at}$ is the mass of metal atoms. In step (ii), no energy dissipation channel is provided, and thus, there is no damping coefficient involved in the rigid body motion of the tip. Therefore, the damping coefficient (γ) or the viscous friction coefficient (μ) in the PT model (1) must be tied to the intrinsic relaxation rate of the atomic system. We now can further assume that only γ is tied to this relaxation rate, while the viscous friction coefficient $\mu = 2\gamma \sqrt{k/m}$ depends not only on γ but also on the tip mass m. To further illustrate this point, in Figure S3 (see the Supporting Information), we show three stick-slip friction traces obtained from the two-step MD simulations for the same Pt tip (i.e., $m_{tip} = 100$ Au mass for all

three cases). The first friction trace corresponds to the atomic relaxation in step (i) where both Au and Pt atoms hold the actual atomic mass (i.e., $m_{\rm Au} = 197$ and $m_{\rm Pt} = 195$ amu), the second friction trace corresponds to the atomic relaxation in step (i) where the Pt atomic mass takes the reduced mass (i.e., $m_{\rm Au}$ = 197 and $m_{\rm Pt}$ = 1.07 amu), and the third friction trace corresponds to both Au and Pt atoms taking the reduced atomic mass (i.e., $m_{Au} = m_{Pt} = 1.07$ amu). Figure S3 shows that the fast relaxation dynamics of the light particles result in lower frictions than those from actual atomic mass relaxations. Since the same tip mass ($m_{\text{tip}} = 100 \text{ Au mass}$) was used in step (ii) for all three cases, the difference in friction forces calculated is clearly relevant to the relaxation rate of the atomic system. This suggests that the damping coefficient (γ) in the PT model should be an intrinsic constant that must be tied to the atomic relaxation in the two-step MD simulations.

Knowing that the amplitude of the corrugation potential U is linearly related to the maximum lateral friction force, 46 we found that U can be fitted by the mean value of this maximum friction force from MD simulations (Figure 6) under the normal load of N_{ext} = 0.6 nN, yielding U = 1.5 eV. To determine the damping coefficient γ , we noticed that because the governing equation of the PT model is a stochastic differential equation and the friction traces that the model generated fluctuates statistically, our choice of fitting this parameter is to make sure that the reproduced stick-slip friction traces and tip displacements are qualitatively similar to the MD simulation results (Figure 6). We thus varied the value of γ and run 50 numerical simulations for each tip with different mass. For each run, we recorded the number of double slips in the stick-slip friction and checked if the number matched the MD simulation results. The most probable γ was determined corresponding to the largest probability of the occurrence of MD double stick slips (see

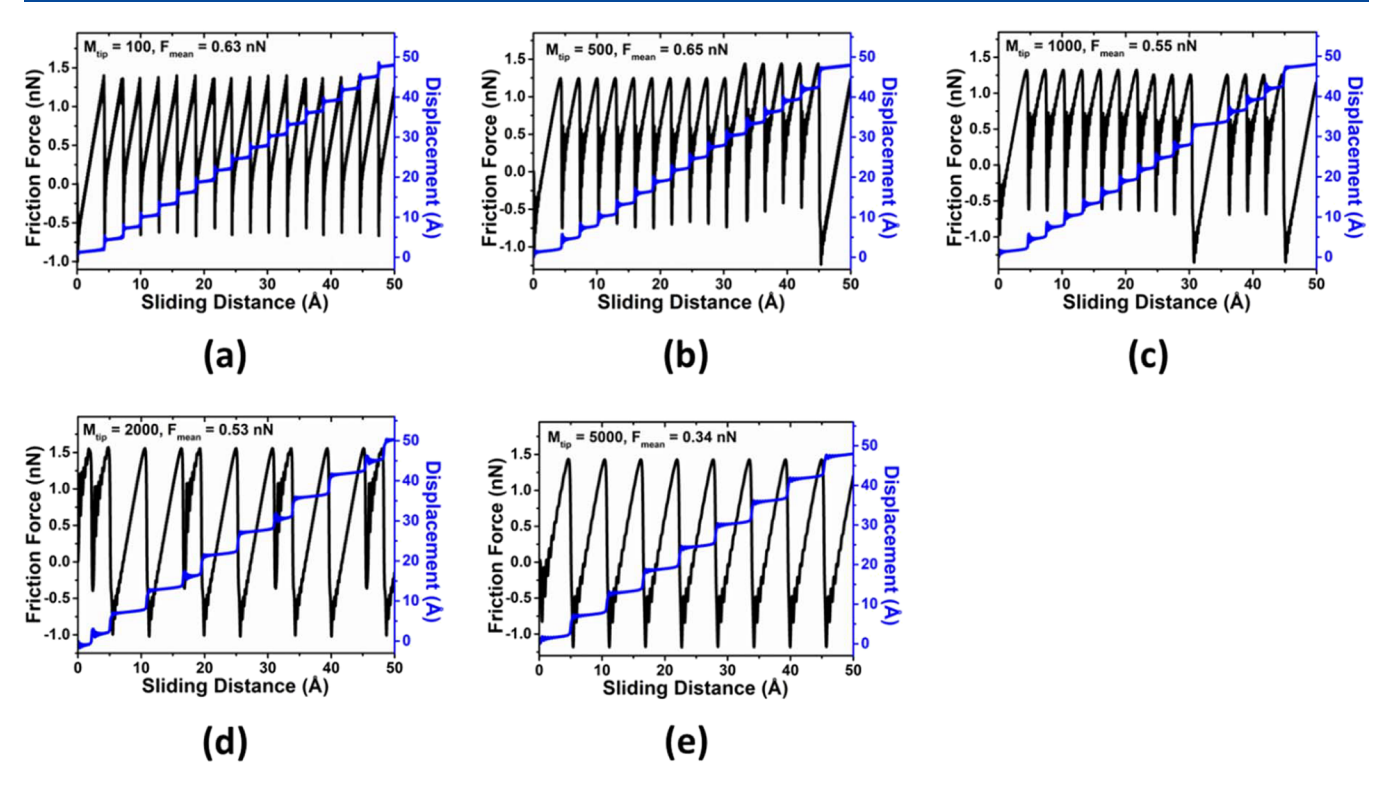


Figure 7. Variations of stick—slip friction force and tip displacement versus the sliding distance of the driving spring predicted by the PT model. Here, for the same tip mass varying from (a) $m_{\text{tip}} = 100$ gold atomic mass to (e) $m_{\text{tip}} = 5000$ gold atomic mass, the relevant parameters used in the PT model were chosen to be consistent with MD simulations.

Table S1 in the Supporting Information). Based on this statistical approach, we found that $\gamma=0.16$ is a suitable value, which corresponds to an underdamped situation often observed in AFM friction measurements. Other relevant parameters used in the PT model were chosen to be consistent with MD simulations: a=0.28 nm, k=6 N/m, v=1 m/s, and T=293 K. By changing the tip mass from $m_{\rm tip}=100$ to $m_{\rm tip}=5000$ atomic masses of gold, we showed in Figure 7 the stick—slip friction transitions from single slips to double slips beginning at the $m_{\rm tip}=500$ Au mass tip, which are qualitatively consistent with the MD simulation results shown in Figure 6.

It is worth noting that a previous theoretical study using the PT model showed that the damping coefficient (γ) had a direct effect on the mode of atomic stick—slip friction. ⁴⁵ Here, we demonstrate that one of the origins of this damping is associated with the atomic relaxation rate ($r_{\rm at}$) of the system. Specifically, even for the same damping (γ), the dynamic tip mass $m_{\rm tip}$ has a profound effect on the mode of stick—slip friction. This result is surprisingly similar to the findings by van Baarle and Krylov et al., ⁴¹ who used a two-mass—two-spring model to show that increasing the dynamic mass of the tip apex would induce multiple-slip events.

A simple quasi-static friction analysis showed that the PT model could predict two different modes for the tip motion depending on the dimensionless parameter $\eta = \frac{2\pi^2 U}{a^2 k}$, which represents the ratio between the stiffness of the tip—substrate potential and the driving spring. And Quick calculation showed that this parameter was close to 10, satisfying $\eta > 4.6$ for the possible slips of multiplicity (multiple-slip regime). However, transitions between different friction regimes were ultimately determined by the dynamic friction, as elaborated by Dong et al., who focused on three relevant parameters: damping of

the system, sliding speed, and temperature. Here, we point out that the additional mass-dependent stick—slip transition from single slips to double slips could be further explained from three possible aspects: First, for the same underdamped system ($\gamma=0.16$), increasing the tip mass m will decrease the actual friction coefficient μ of the tip in Langevin dynamics (1), resulting in possible double slips; second, according to the two-mass—two-spring model, assuming the atomic motions are critically damped, increasing the dynamic mass of the tip apex while keeping the same number of contact atoms will bring the system into an underdamped situation, resulting in multiple-slip events; finally, such a mass-dependent friction transition may relate to the attempt frequency f_0 of the slip due to thermal activations, which were given by 45

$$f_0 = \left(\left(\frac{\mu^2}{4} + \omega_{\rm t}^2 \right)^{1/2} - \frac{\mu}{2} \right) \frac{\omega_{\rm i}}{2\pi\omega_{\rm t}},\tag{4}$$

where $\omega_{\rm i}^2=V''(x_{\rm i})/m$ is the squared angular frequency at the metastable minimum $x_{\rm i}$, and $\omega_{\rm t}^2=V''(x_{\rm t})/m$ denotes the squared angular frequency at the transition point $x_{\rm t}$. Equation 4 shows that increasing the tip mass m will decrease the attempt frequency f_0 , resulting in delayed slip-through thermal activations. As such, the slip jump at a delayed stage through thermal activation will result in more potential energy accumulated so that the net energy needs to be dissipated during the slip can be larger, 45 leading to multiple slips.

4. CONCLUSIONS

The present MD simulation studies of a 10 nm radius polycrystalline Pt tip sliding on a gold(111) surface provide and reveal the following insights into the stick—slip friction observed in AFM experiments:

- (1). If the apex of an AFM tip has multiple neighboring grains involved in the sliding contact, using such an AFM tip can induce severe plastic deformation of the metal substrate during sliding, resulting in irregular stick—slip high friction.
- (2). However, regular stick—slip friction with single atomic slips could be achieved when the AFM tip apex adopts a single crystalline protrusion without any neighboring grains involved in the contact. Such regular stick—slip fiction with single slip signals will be quite tolerant to the adhesion of a large number of gold atoms on the periphery of the AFM tip apex.
- (3). In MD simulations of friction in AFM, the effective tip mass plays an important role in determining the transition between friction regimes. As the effective mass of the tip increases, the stick—slip friction could be changed from the single-slip to the multiple-slip regime.

A previous experimental study showed that transitions from the single-slip to the multiple-slip regime in atomic-scale friction depend on the lateral stiffness of the coupled tip—substrate system and contact load, 32 while the effective mass of the AFM tip—cantilever system is constantly around 10^{-11} kg. 20,21 In MD simulations, however, one should keep in mind that properly selecting a dynamic inertia of the model tip is not only a matter of choice but also an important control parameter in order to capture the critical dynamics and energetics of AFM friction measurements.

ASSOCIATED CONTENT

Supporting Information

The Supporting Information is available free of charge at https://pubs.acs.org/doi/10.1021/acs.langmuir.1c03268.

Additional snapshots of dislocation distributions in polycrystalline Pt tip and Au substrate; variations of stick—slip friction traces versus atomic relaxation rate changes by artificially changing the atomic mass for both Au and Pt atoms; probability of the occurrence of double slips for different damping coefficient and tip mass (PDF)

AUTHOR INFORMATION

Corresponding Author

Yongsheng Leng — Department of Mechanical and Aerospace Engineering, The George Washington University, Washington, DC 20052, United States; ⊚ orcid.org/0000-0002-3558-5016; Email: leng@gwu.edu

Author

Rong-Guang Xu — Department of Mechanical and Aerospace Engineering, The George Washington University, Washington, DC 20052, United States; orcid.org/0000-0002-0716-5831

Gunan Zhang – Department of Mechanical and Aerospace Engineering, The George Washington University, Washington, DC 20052, United States

Yuan Xiang – Department of Mechanical and Aerospace Engineering, The George Washington University, Washington, DC 20052, United States; ○ orcid.org/0000-0002-4665-3360

Jonathan Garcia – Department of Mechanical and Aerospace Engineering, The George Washington University, Washington, DC 20052, United States Complete contact information is available at: https://pubs.acs.org/10.1021/acs.langmuir.1c03268

Notes

The authors declare no competing financial interest.

ACKNOWLEDGMENTS

This work was supported by the National Science Foundation (NSF 1953171) and the resources of the National Energy Research Scientific Computing Center (NERSC), a DOE Office of Science User Facility supported by the Office of Science of the U. Department of Energy under contract no. DE-AC02-05CH11231.

REFERENCES

- (1) Binnig, G.; Quate, C. F.; Gerber, C. Atomic force microscope. *Phys. Rev. Lett.* **1986**, 56, 930–933.
- (2) Mate, C. M.; McClelland, G. M.; Erlandsson, R.; Chiang, S. Atomic-scale friction of a tungsten tip on a graphite surface. *Phys. Rev. Lett.* **1987**, *59*, 1942–1945.
- (3) Szlufarska, I.; Chandross, M.; Carpick, R. W. Recent advances in single-asperity nanotribology. *J. Phys. D: Appl. Phys.* **2008**, *41*, 123001.
- (4) Vanossi, A.; Manini, N.; Urbakh, M.; Zapperi, S.; Tosatti, E. Colloquium: Modeling friction: From nanoscale to mesoscale. *Rev. Mod. Phys.* **2013**, *85*, 529–552.
- (5) Urbakh, M.; Meyer, E. Nanotribology: The renaissance of friction. *Nat. Mater.* **2010**, *9*, 8–10.
- (6) Harrison, J. A.; White, C. T.; Colton, R. J.; Brenner, D. W. Molecular dynamic simulations of atomic-scale friction of diamond surfaces. *Phys. Rev. B* **1992**, *46*, 9700–9708.
- (7) Luan, B.; Robbins, M. O. The breakdown of continuum models for mechanical contacts. *Nature* **2005**, *435*, 929–932.
- (8) Mo, Y.; Turner, K. T.; Szlufarska, I. Friction laws at the nanoscale. *Nature* **2009**, *457*, 1116–1119.
- (9) Gnecco, E.; Bennewitz, R.; Gyalog, T.; Loppacher, C.; Bammerlin, M.; Meyer, E.; Güntherodt, H.-J. Velocity dependence of atomic friction. *Phys. Rev. Lett.* **2000**, 84, 1172–1175.
- (10) Sang, Y.; Dubé, M.; Grant, M. Thermal effects on atomic friction. *Phys. Rev. Lett.* **2001**, *87*, 174301.
- (11) Riedo, E.; Gnecco, E.; Bennewitz, R.; Meyer, E.; Brune, H. Interaction potential and hopping dynamics governing sliding friction. *Phys. Rev. Lett.* **2003**, *91*, No. 084502.
- (12) Muser, M. H.; Urbakh, M.; Robbins, M. O. Statistical mechanics of static and low-velocity kinetic friction. In *Advances in Chemical Physics, Vol* 126; John Wiley & Sons Inc: New York, 2003; Vol. 126, pp. 187–272.
- (13) Sorensen, M. R.; Jacobsen, K. W.; Stoltze, P. Simulations of atomic-scale sliding friction. *Phys. Rev. B* **1996**, *53*, 2101–2113.
- (14) Filippov, A. E.; Klafter, J.; Urbakh, M. Friction through dynamical formation and rupture of molecular bonds. *Phys. Rev. Lett.* **2004**, 92, 4.
- (15) Gao, G.; Cannara, R. J.; Carpick, R. W.; Harrison, J. A. Atomic-scale friction on diamond: A comparison of different sliding directions on (001) and (111) surfaces using MD and AFM. *Langmuir* **2007**, 23, 5394–5405.
- (16) Sinnott, S. B.; Colton, R. J.; White, C. T.; Shenderova, O. A.; Brenner, D. W.; Harrison, J. A. Atomistic simulations of the nanometer-scale indentation of amorphous-carbon thin films. *J. Vac. Sci. Technol., A* **1997**, *15*, 936–940.
- (17) Leng, Y.; Jiang, S. Atomic indentation and friction of self-assembled monolayers by hybrid molecular simulations. *J. Chem. Phys.* **2000**, *113*, 8800–8806.
- (18) Leng, Y.; Jiang, S. Dynamic simulations of adhesion and friction in chemical force microscopy. *J. Am. Chem. Soc.* **2002**, *124*, 11764–11770.

- (19) Martini, A.; Dong, Y.; Perez, D.; Voter, A. F. Low-Speed Atomistic Simulation of Stick-Slip Friction using Parallel Replica Dynamics. *Tribol. Lett.* **2009**, *36*, 63–68.
- (20) Li, Q.; Dong, Y.; Perez, D.; Martini, A.; Carpick, R. W. Speed Dependence of Atomic Stick-Slip Friction in Optimally Matched Experiments and Molecular Dynamics Simulations. *Phys. Rev. Lett.* **2011**, *106*, 126101.
- (21) Liu, X.-Z.; Ye, Z.; Dong, Y.; Egberts, P.; Carpick, R. W.; Martini, A. Dynamics of Atomic Stick-Slip Friction Examined with Atomic Force Microscopy and Atomistic Simulations at Overlapping Speeds. *Phys. Rev. Lett.* **2015**, *114*, 146102.
- (22) Leng, Y. S.; Jiang, S. Slow dynamics in atomic-force microscopy. *Phys. Rev. B* **2001**, *63*, 193406.
- (23) Plimpton, S. Fast parallel algorithms for short-range molecular-dynamics. *J. Comput. Phys.* **1995**, *117*, 1–19.
- (24) Bennewitz, R.; Hausen, F.; Gosvami, N. N. Nanotribology of clean and modified gold surfaces. *J. Mater. Res.* **2013**, 28, 1279–1288.
- (25) Gosvami, N. N.; Feldmann, M.; Peguiron, J.; Moseler, M.; Schirmeisen, A.; Bennewitz, R. Ageing of a Microscopic Sliding Gold Contact at Low Temperatures. *Phys. Rev. Lett.* **2011**, *107*, 144303.
- (26) Gosvami, N. N.; Filleter, T.; Egberts, P.; Bennewitz, R. Microscopic Friction Studies on Metal Surfaces. *Tribol. Lett.* **2010**, 39, 19–24.
- (27) Comtet, J.; Lainé, A.; Niguès, A.; Bocquet, L.; Siria, A. Atomic rheology of gold nanojunctions. *Nature* **2019**, *569*, 393–397.
- (28) Ko, H. E.; Kwan, S. G.; Park, H. W.; Caron, A. Chemical effects on the sliding friction of Ag and Au(111). *Friction* **2018**, *6*, 84–97.
- (29) Vishnubhotla, S. B.; Chen, R.; Khanal, S. R.; Martini, A.; Jacobs, T. D. B. Understanding contact between platinum nanocontacts at low loads: The effect of reversible plasticity. *Nanotechnology* **2018**, *30*, No. 035704.
- (30) He, Y.; She, D.; Liu, Z.; Wang, X.; Zhong, L.; Wang, C.; Wang, G.; Mao, S. X. Atomistic observation on diffusion-mediated friction between single-asperity contacts. *Nat. Mater.* **2022**, *21*, 173–180.
- (31) Dong, Y.; Li, Q.; Martini, A. Molecular dynamics simulation of atomic friction: A review and guide. *J. Vac. Sci. Technol., A* **2013**, *31*, No. 030801.
- (32) Medyanik, S. N.; Liu, W. K.; Sung, I.-H.; Carpick, R. W. Predictions and Observations of Multiple Slip Modes in Atomic-Scale Friction. *Phys. Rev. Lett.* **2006**, *97*, 136106.
- (33) Voter, A. F. Embedded Atom Method Potentials for seven FCC metals: Ni, Pd, Pt, Cu, Ag, Au, and Al. Los Alamos Unclassified Technical Report # LA-UR 93–3901; 1993.
- (34) Nosé, S. A unified formulation of the constant temperature molecular dynamics methods. *J. Chem. Phys.* **1984**, *81*, 511–519.
- (35) Hoover, W. G. Canonical dynamics: Equilibrium phase-space distributions. *Phys. Rev. A* 1985, 31, 1695.
- (36) Stukowski, A. Visualization and analysis of atomistic simulation data with OVITO—the Open Visualization Tool. *Modell. Simul. Mater. Sci. Eng.* **2009**, *18*, No. 015012.
- (37) Sommerfeld, D. A.; Cambron, R. T.; Beebe, T. P. Topographic and diffusion measurements of gold and platinum surfaces by scanning tunneling microscopy. *J. Phys. Chem.* **1990**, *94*, 8926–8932.
- (38) Larsen, P. M.; Schmidt, S.; Schiøtz, J. Robust structural identification via polyhedral template matching. *Modell. Simul. Mater. Sci. Eng.* **2016**, 24, No. 055007.
- (39) Stukowski, A.; Albe, K. Extracting dislocations and non-dislocation crystal defects from atomistic simulation data. *Modell. Simul. Mater. Sci. Eng.* **2010**, *18*, No. 085001.
- (40) Stukowski, A.; Bulatov, V. V.; Arsenlis, A. Automated identification and indexing of dislocations in crystal interfaces. *Modell. Simul. Mater. Sci. Eng.* **2012**, *20*, No. 085007.
- (41) van Baarle, D. W.; Krylov, S. Y.; Beck, M. E. S.; Frenken, J. W. M. On the Non-trivial Origin of Atomic-Scale Patterns in Friction Force Microscopy. *Tribol. Lett.* **2019**, *67*, 15.
- (42) Sharp, T. A.; Pastewka, L.; Lignères, V. L.; Robbins, M. O. Scale- and load-dependent friction in commensurate sphere-on-flat contacts. *Phys. Rev. B* **2017**, *96*, 155436.

- (43) Prandtl, L. A conceptual model to the kinetic theory of solid bodies. Z. Angew. Math. Mech. 1928, 8, 85–106.
- (44) Tomlinson, G. A. A molecular theory of friction. *Phil. Mag.* **1929**, 7, 905–939.
- (45) Dong, Y.; Vadakkepatt, A.; Martini, A. Analytical Models for Atomic Friction. *Tribol. Lett.* **2011**, *44*, 367.
- (46) Socoliuc, A.; Bennewitz, R.; Gnecco, E.; Meyer, E. Transition from Stick-Slip to Continuous Sliding in Atomic Friction: Entering a New Regime of Ultralow Friction. *Phys. Rev. Lett.* **2004**, *92*, 134301.

□ Recommended by ACS

Cross-Sectional Imaging of Boundary Lubrication Layer Formed by Fatty Acid by Means of Frequency-Modulation Atomic Force Microscopy

Tomoko Hirayama, Hiroshi Onishi, et al.

SEPTEMBER 29, 2017

LANGMUIR

READ 🗹

Adsorption Behavior and Nanotribology of Amine-Based Friction Modifiers on Steel Surfaces

Prathima C. Nalam, Rosa M. Espinosa-Marzal, et al.

MAY 07, 2019

THE JOURNAL OF PHYSICAL CHEMISTRY C

READ 🗹

Characterization of Repulsive Forces and Surface Deformation in Thin Micellar Films via AFM

Benjamin L. Micklavzina and Marjorie L. Longo

SEPTEMBER 13, 2017

LANGMUIR

READ 🗹

Lubrication of Si-Based Tribopairs with a Hydrophobic Ionic Liquid: The Multiscale Influence of Water

Andrea Arcifa, Nicholas D. Spencer, et al.

MARCH 16, 2018

THE JOURNAL OF PHYSICAL CHEMISTRY C

READ 🗹

Get More Suggestions >